

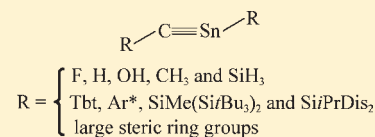
Triply Bonded Stannaacetylene (RC≡SnR): Theoretical Designs and Characterization

Po-Chao Wu and Ming-Der Su*

Department of Applied Chemistry, National Chiayi University, Chiayi 60004, Taiwan

Supporting Information

ABSTRACT: The effect of substitution on the potential energy surfaces of RC≡SnR (R = F, H, OH, CH₃, SiH₃, Tbt, Ar*, SiMe(Si^tBu₃)₂, and SiⁱPrDis₂) was explored using density functional theories (B3LYP/LANL2DZdp and B3PW91/Def2-QZVP). Our theoretical investigations indicate that all the triply bonded RC≡SnR molecules prefer to adopt a trans-bent geometry, which is in good agreement with the theoretical model (mode B). In addition, we demonstrate that the stabilities of the RC≡SnR compounds bearing smaller substituents (R = F, H, OH, CH₃, and SiH₃) decrease in the order R₂C=Sn: > RC≡SnR > :C=SnR₂. On the other hand, the triply bonded R'C≡SnR' molecules with bulkier substituents (R' = Tbt, Ar*, SiMe(Si^tBu₃)₂, and SiⁱPrDis₂) were found to possess the global minimum on the singlet potential energy surface and are both kinetically and thermodynamically stable. Further, we used the B3LYP computations to predict the stability of stannaacetylene bearing the very bulky phosphine ligand. Our theoretical observations strongly suggest that both the electronic and the steric effects of bulky substituents play an important role in making triply bonded stannaacetylene (RC≡SnR) an intriguing synthetic target.



I. INTRODUCTION

The search for triply bonded structures containing group 14 elements has received increasing attention from both experimentalists and theoreticians,¹ due to the potentially unique properties of these structures as well as the importance of academic research. The homonuclear combinations $-M\equiv M-$ (M = C, Si, Ge, Sn, and Pb) are well known up to now; many compounds of this type have been synthesized and fully characterized.^{2–5} The progress in this field is apparently reflected by the large number of reviews published during the past decade.¹ Nevertheless, the synthesis and isolation of heteronuclear alkyne analogues, stable combinations between the different heavier group 14 elements $-M\equiv M'-$, have received comparatively very little attention. To the best of our knowledge, so far the chemistry of heteronuclear heavy alkynes was limited only to such combinations where one carbon atom of ethyne has been replaced by a heavier element of group 14, that is, silaacetylene ($-C\equiv Si-$)⁶ and germaacetylene ($-C\equiv Ge-$).⁷ In fact, heteronuclear combinations having two different triply bonded group 14 elements $-M\equiv M'-$ should be of particular importance because they provide a much greater variation in the bonding schemes than the symmetrical homonuclear molecules $-M\equiv M-$ based on the nature of the two triply bonded elements such as electronegativity and polarizability.

Recently, Sakamoto, Kira, and co-workers reported the first evidence for the successful generation of a short-lived stannaacetylene $R_3SiC\equiv SnAr$ (R = *i*-Pr and Ar = 2,6-Tip₂-C₃H₆-) via photolysis of the corresponding diazomethylstannylenes.⁸ Until now, however, no X-ray diffraction data for this species has been obtained. The scarce experimental information on such a molecule is mainly due to the significantly decreased stability of the carbon–tin triple bond, that is, the electronegativity difference ($\chi(C) - \chi(Sn) = 0.8$)⁹ results in the carbon–tin π system being

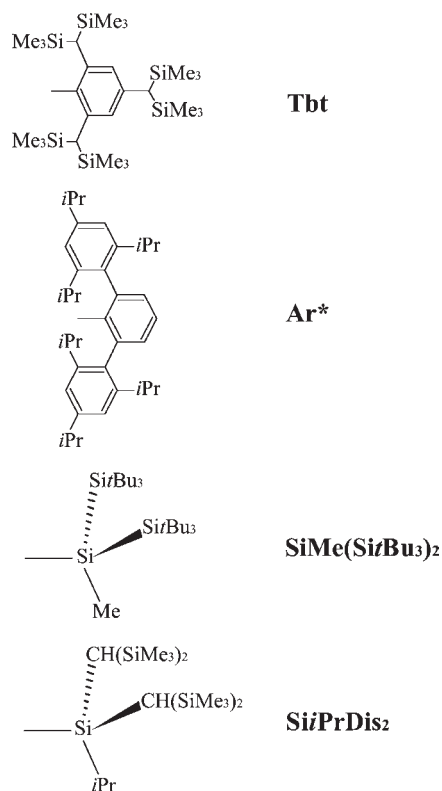
rather polarized. Such polarization can further increase the reactivity of the molecules possessing the C≡Sn triple bond, which often leads to facile decomposition to tin-containing precipitates. This, in turn, severely complicates their synthesis and characterization. As a result of the experimental difficulties in handling these molecules, the nature of their bonding and their X-ray structures are still not as well understood at this time as other analogues. In fact, to our knowledge, until now neither experimental nor theoretical studies have been performed on these systems. Indeed, it is astonishing how little is known about the stability and molecular properties of stannaacetylenes (RC≡SnR), considering the importance of carbon–tin in synthetic chemistry¹⁰ and the extensive research activity related to the corresponding acetylene and silaacetylene species.⁶

The question whether triply bonded stannaacetylenes can be synthesized as stable compounds when they are properly substituted is an interesting one. However, no research has been discussed about such substituent effects on the molecular systems containing the carbon–tin triple bond; we thus report for the first time in the literature the structures of stannaacetylene with various substituents, that is, we have undertaken theoretical calculations of RC≡SnR utilizing both smaller ligands (such as, R = F, H, OH, CH₃, and SiH₃) and larger ligands having bulky aryl and silyl groups (i.e., R' = Tbt, Ar*, SiMe(Si^tBu₃)₂, and SiⁱPrDis₂; Dis = CH(SiMe₃)₂; Scheme 1) as well as the sterically bulky ring groups.^{6c,d} As a result, the effect of substituents on such carbon–tin triple bonds has been systematically investigated by performing density functional theory (DFT) calculations. It is our aim that the theoretical interpretations of substituent

Received: May 3, 2011

Published: June 21, 2011

Scheme 1



effects presented in this work will be greatly helpful in preparing the fruitful precursors of stannaacetylenes.

II. THEORETICAL METHODS

Geometries were fully optimized with hybrid density functional theory at both the B3LYP and the B3PW91 levels using the Gaussian 03 program package.¹¹ In both the B3LYP and B3PW91 calculations, Becke's 3-parameter nonlocal exchange functional (B3)¹² was used together with the exact (Hartree–Fock) exchange functional in conjunction with the nonlocal correlation functional of Lee, Yang, and Parr (LYP)¹³ and Perdew and Wang (PW91).¹⁴ Thus, the geometries of all the stationary points were fully optimized at the B3LYP and B3PW91 levels of theory. These B3LYP calculations were carried out with pseudorelativistic effective core potentials on group 14 elements modeled using the double- ζ (DZ) basis sets¹⁵ augmented by a set of d-type polarization functions.¹⁶ The DZ basis set for the hydrogen element was augmented by a set of p-type polarization functions (p exponents 0.356). The d exponents used for C, Si, Ge, Sn, and Pb were 0.587, 0.296, 0.246, 0.186, and 0.179, respectively. Accordingly, we denote our B3LYP calculations by B3LYP/LANL2DZdp. Moreover, the geometries and energetics of the stationary points on the potential energy surface were also calculated using the B3PW91 method in conjunction with the Def2-QZVP basis set.¹⁷ Consequently, we denote our B3PW91 calculations by B3PW91/Def2-QZVP.

The spin-unrestricted (UB3LYP and UB3PW91) formalisms were used for the open-shell (doublet and quartet) species. The S^2 expectation values of the doublet and quartet states for the calculated species all showed an ideal value (0.75 and 3.75, respectively) after spin annihilation, so that their geometries and

energetics are reliable for this study. Frequency calculations were performed on all structures to confirm that the reactants and products had no imaginary frequencies and that the transition states possessed only one imaginary frequency. The relative energies were thus corrected for vibrational zero-point energies (ZPE, not scaled).

On the other hand, sequential conformation analyses were carried out for each stationary point for species containing bulky ligands ($R' = \text{Tbt}, \text{Ar}^*, \text{SiMe}(\text{Si}t\text{Bu}_3)_2$, and $\text{Si}i\text{PrDis}_2$) using Hartree–Fock calculations (RHF/3-21G*). Thus, the model reactants have 998 (666 electrons), 892 (586 electrons), 840 (554 electrons), and 724 (490 electrons) basis functions for $\text{Tbt}-\text{C}\equiv\text{Sn}-\text{Tbt}$, $\text{Ar}^*-\text{C}\equiv\text{Sn}-\text{Ar}^*$, $\text{SiMe}(\text{Si}t\text{Bu}_3)_2-\text{C}\equiv\text{Sn}-\text{SiMe}(\text{Si}t\text{Bu}_3)_2$, and $\text{Si}i\text{PrDis}_2-\text{C}\equiv\text{Sn}-\text{Si}i\text{PrDis}_2$, respectively. It is well known that the Hartree–Fock level of theory is insufficient for even a qualitative description of the chemical potential energy surface. Thus, these stationary points were then further calculated at the B3LYP/LANL2DZdp level using the opt=readfc keyword with a tight convergence option (maximum gradient convergence tolerance = 5.0×10^{-5} hartree/bohr). Due to the limitation of both CPU time and memory size available, frequencies were not calculated for the triply bonded $\text{R}'\text{C}\equiv\text{SnR}'$ systems with bulky ligands at the B3LYP/LANL2DZdp level of theory. As a result, the ZPE of B3LYP/LANL2DZdp could not be applied to such systems.

Furthermore, we also investigated another kind of substituent effect using the very bulky phosphine ligand mentioned by Kato, Bacciredo, and co-workers (vide infra).^{6c} However, complete calculations for such systems that were studied experimentally are prohibitively expensive. To reduce the computational time as well the disk space, we thus used the B3LYP/LANL2DZ method to explore their relative stability of the triply bonded carbon–tin systems. Vibrational frequencies at stationary points were calculated at the B3LYP/LANL2DZ level of theory to identify them as minima (zero imaginary frequencies) or transition states (one imaginary frequency). The relative energies were therefore corrected for vibrational zero-point energies (ZPE, not scaled). The Cartesian coordinates calculated for all the stationary points studied in this work at the B3LYP/LANL2DZdp, B3PW91/Def2-QZVP, and B3LYP/LANL2DZ levels of theory are available as Supporting Information.

III. RESULTS AND DISCUSSION

1. Theoretical Models for $\text{RC}\equiv\text{SnR}$. It is instructive to view $\text{R}-\text{C}\equiv\text{Sn}-\text{R}$ as being composed of one $\text{C}-\text{R}$ and one $\text{Sn}-\text{R}$ unit. Thus, formation of $\text{R}-\text{C}\equiv\text{Sn}-\text{R}$ species from the two fragments can be regarded as a bonding process that is illustrated schematically in Figure 1. As can be seen in Figure 1, there are two possible interaction modes (A and B) between the $\text{C}-\text{R}$ and the $\text{Sn}-\text{R}$ moieties in forming the triply bonded species. In model A, both $\text{C}-\text{R}$ and $\text{Sn}-\text{R}$ units exist as quartet monomers.¹⁸ In this way, the combination between carbon and tin can be considered a triple bond since it consists of overlapping the singly occupied orbitals of these two quartet monomers. As a result, this bonding model can lead to a linear structure as shown in Figure 1A. On the other hand, in model B, both $\text{C}-\text{R}$ and $\text{Sn}-\text{R}$ units exist as doublets. Thus, this bonding scheme contains two donor–acceptor as well as polar–dative bonds involving the lone pairs (indicated by arrows) plus a π bond owing to coupling between the unpaired electron in the p orbital on each carbon and tin element (indicated by a dashed line). Accordingly, this

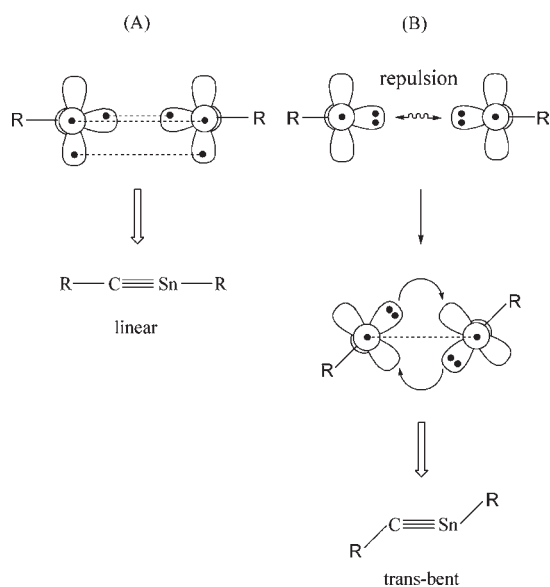


Figure 1. Two interaction models, A and B, in forming triply bonded group 14 $\text{RC}\equiv\text{SnR}$ species.

bonding pattern can result in a trans-bent structure as given in Figure 1B. Bearing these analyses in mind, we shall utilize them to explain the geometrical structures of triply bonded $\text{RC}\equiv\text{SnR}$ species in the following sections.

2. Small Ligands on Substituted $\text{RC}\equiv\text{SnR}$. In this section, the small ligands, such as $\text{R} = \text{F}, \text{H}, \text{OH}, \text{CH}_3,$ and SiH_3 , were first chosen to study the geometries of the $\text{RC}\equiv\text{SnR}$ species. Since to date neither experimental nor theoretical parameters for such triple-bonded compounds are available for comparison, we use two kinds of DFT methods (i.e., B3LYP/LANL2DZdp and B3PW91/Def2-QZVP) to examine their molecular properties. The selected geometrical parameters, doublet–quartet energy splitting ($\Delta E_{\text{DQ}} = E_{\text{quartet}} - E_{\text{doublet}}$), natural charge densities (Q_{C} and Q_{Sn}), and binding energies (BE) are summarized in Table 1.

As seen in Table 1, the geometrical parameters of the $\text{RC}\equiv\text{SnR}$ triply bonded molecules are quite similar at both DFT levels employed. For instance, one of the intriguing structural features of the $\text{RC}\equiv\text{SnR}$ species is the $\text{C}\equiv\text{Sn}$ bond length. In the parent $\text{HC}\equiv\text{SnH}$ molecule, the carbon–tin bond distance is 1.926 and 1.902 Å, respectively, at the B3LYP and B3PW91 levels of theory. The data in Table 1 demonstrate that the $\text{C}\equiv\text{Sn}$ bond lengths, which fall in the range of 1.926–2.127 and 1.896–2.117 Å, respectively, change quite significantly upon substitution. As stressed earlier, no $\text{C}\equiv\text{Sn}$ triple-bond distances have been reported so far, both experimentally and theoretically.^{8,19–21} Moreover, on the basis of the present work shown in Table 1, one can see that highly electronegative substituents at carbon and tin elements lengthen the $\text{C}\equiv\text{Sn}$ bond relative to $\text{HC}\equiv\text{SnH}$, whereas electropositive substituents result in a shortening $\text{C}\equiv\text{Sn}$ bond distance. The reason for the substituents on the $\text{C}\equiv\text{Sn}$ triple-bond length can be understood easily in terms of bond polarity. As already mentioned in the Introduction,⁹ the electronegativity of carbon ($x = 2.5$) and tin ($x = 1.7$) elements are different so that the carbon atom is negatively charged and the tin is positively charged, i.e., $\text{R}-\text{C}^{\ominus}\equiv\text{Sn}^{\oplus}-\text{R}$. Accordingly, substituents that increase this polarization and thus the degree of ionicity of the $\text{C}\equiv\text{Sn}$ triple bond are expected to shorten this

Table 1. Selected Geometrical Parameters, Doublet–Quartet Energy Splitting (ΔE_{DQ}), Natural Charge Densities (Q_{C} and Q_{Sn}), and Binding Energies (BE) of $\text{RC}\equiv\text{SnR}$ at the B3LYP/LANL2DZdp and B3PW91/Def2-QZVP Levels

R	F	H	OH	CH_3	SiH_3
B3LYP/LANL2DZdp					
$\text{C}\equiv\text{Sn}$ (Å)	2.081	1.926	2.127	1.966	1.934
$\angle\text{R}-\text{C}-\text{Sn}$ (deg)	151.5	146.1	142.0	159.9	160.3
$\angle\text{C}-\text{Sn}-\text{R}$ (deg)	100.6	116.5	93.04	107.9	111.1
$\angle\text{R}-\text{C}-\text{Sn}-\text{R}$ (deg)	178.9	179.9	105.1	177.2	177.3
Q_{C}^a	-0.2340	-0.4904	-0.3258	-0.4686	-0.4887
Q_{Sn}^b	0.7784	0.4725	0.5455	0.3003	0.1915
ΔE_{DQ} for C (kcal mol ⁻¹) ^c	82.08	20.51	86.09	35.46	1.490
ΔE_{DQ} for Sn (kcal mol ⁻¹) ^d	86.34	45.24	77.79	43.48	31.39
BE (kcal mol ⁻¹) ^e	28.02	70.26	29.81	58.98	82.79
B3PW91/Def2-QZVP					
$\text{C}\equiv\text{Sn}$ (Å)	2.076	1.902	2.117	1.953	1.896
$\angle\text{R}-\text{C}-\text{Sn}$ (deg)	147.6	139.8	144.8	155.8	151.0
$\angle\text{C}-\text{Sn}-\text{R}$ (deg)	102.9	127.5	93.98	112.5	133.4
$\angle\text{R}-\text{C}-\text{Sn}-\text{R}$ (deg)	179.9	177.5	110.2	179.9	179.7
Q_{C}^a	-0.1064	-0.4256	-0.2433	-0.3095	-0.3296
Q_{Sn}^b	0.6479	0.3963	0.5268	0.3793	0.3171
ΔE_{DQ} for C (kcal mol ⁻¹) ^c	76.81	13.45	81.47	30.30	-4.354
ΔE_{DQ} for Sn (kcal mol ⁻¹) ^d	90.70	44.72	78.21	41.63	28.17
BE (kcal mol ⁻¹) ^e	25.42	71.27	28.84	58.58	84.19

^aThe natural charge density on the central carbon atom. ^bThe natural charge density on the central tin atom. ^c $\Delta E_{\text{DQ}} = E(\text{quartet state of C-R}) - E(\text{doublet state of C-R})$. ^d $\Delta E_{\text{DQ}} = E(\text{quartet state of Sn-R}) - E(\text{doublet state of Sn-R})$. ^eBE = $E(\text{doublet state of C-R}) + E(\text{doublet state of Sn-R}) - E(\text{RC}\equiv\text{SnR})$.

bond, as indicated by the natural charge densities on the central carbon and tin elements (Q_{C} and Q_{Sn}) given in Table 1.

In addition, both our DFT calculations demonstrate that both C–R and Sn–R fragments have a doublet ground state, which are more stable than their corresponding quartet states for the small substituents ($\text{R} = \text{F}, \text{H}, \text{OH}, \text{CH}_3,$ and SiH_3), except that the quartet state of C– SiH_3 is lying lower than that of its corresponding doublet state by only 4.4 kcal/mol at the B3PW91/Def2-QZVP level of theory. It is noteworthy that the smaller ΔE_{DQ} values for H and SiH_3 are due to the electropositive character that helps to decrease the size difference between the valence s and p orbitals on the central carbon and tin atoms.²² Accordingly, the two DFT computational results show that all the sum of doublet–quartet energy differences (ΔE_{DQ}) for C–R and Sn–R moieties are at least +33 and +24 kcal/mol for B3LYP and B3PW91 levels of theory. These ΔE_{DQ} values strongly imply that mode B (Figure 1) is prevailing on the $\text{RC}\equiv\text{SnR}$ molecule for which a trans-bent geometry is preferred. This model prediction was confirmed by our present DFT computations, as already presented in Table 1. In addition, as seen in Table 1, the $\text{C}\equiv\text{Sn}$ bond length in $\text{RC}\equiv\text{SnR}$ is strongly correlated with the sum of the doublet–quartet energy (ΔE_{DQ}) of the C–R and the Sn–R units. For instance, our B3LYP computations show that the sum of the ΔE_{DQ} (kcal/mol) values decreases in the order F (168) > OH (164) > CH_3 (78.9) > H (65.8) > SiH_3 (32.9), which follows the similar order as their corresponding triple-bond lengths (Å): OH (2.127) > F (2.081) > CH_3 (1.966) > SiH_3 (1.934) > H (1.926). Likewise, the B3PW91 calculations give that the sum of ΔE_{DQ} (kcal/mol) decreases in the order F (168) > OH (160) > CH_3 (71.9) > H (58.2) > SiH_3 (23.8).

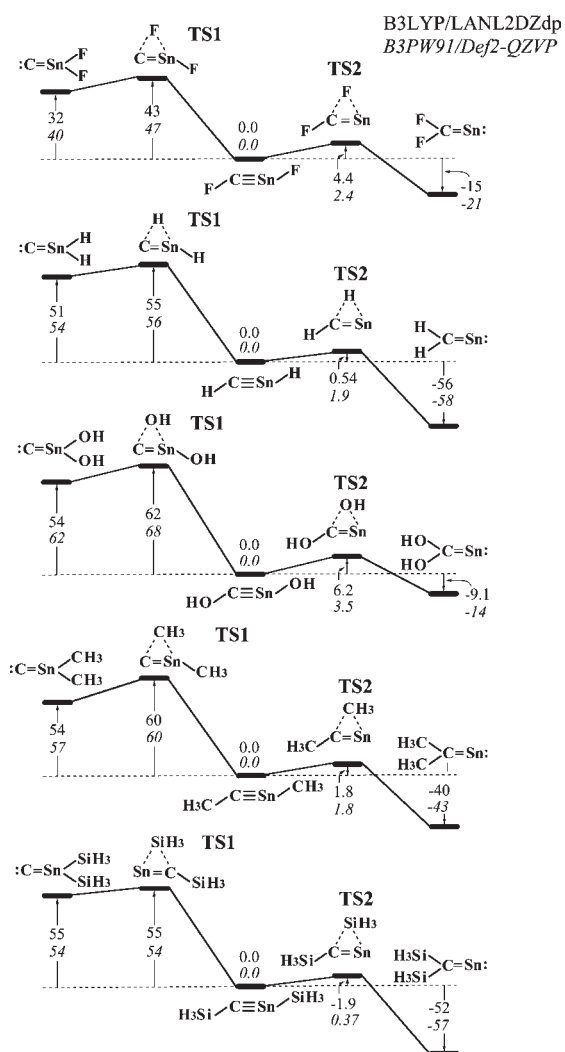


Figure 2. Potential energy surfaces for $RC\equiv SnR$ ($R = F, H, OH, CH_3,$ and SiH_3). Energies are in kcal/mol, calculated at the B3LYP/LANL2DZdp and B3PW91/Def2-QZVP (in parentheses) levels of theory. For details see the text and Table 1. Also see Figure 3 for bulky ligands.

The order of the corresponding triple-bonded distance (Å) follows the same trend as the sum of ΔE_{DQ} : $OH (2.117) > F (2.076) > CH_3 (1.953) > H (1.902) > SiH_3 (1.896)$.

Further, we also consider the binding energies (BE), which can divide the central $C\equiv Sn$ bond into one $C-R$ and one $Sn-R$ units in the doublet ground state. As one can see in Table 1, both B3LYP and B3PW91 computations demonstrate that the BE values are in the range of 28–83 kcal/mol and 25–84 kcal/mol for $R = F, H, OH, CH_3,$ and SiH_3 . These values give strong supporting evidence that the central carbon and tin atoms in these substituted $RC\equiv SnR$ compounds are strongly bonded for the electropositive substituents, compared to the electronegative groups. It has to be pointed out that the above two parameters (the triple-bond distance and ΔE_{DQ}) are strongly dependent on their BE of $RC\equiv SnR$. For example, the BE (kcal/mol) values based on the B3LYP calculations increase in the order $F (28) < OH (30) < CH_3 (59) < H (70) < SiH_3 (83)$. The same situation can also happen at the B3PW91 level of theory (kcal/mol), i.e., $F 3(25) < OH (29) < CH_3 (59) < H (71) < SiH_3 (84)$. In

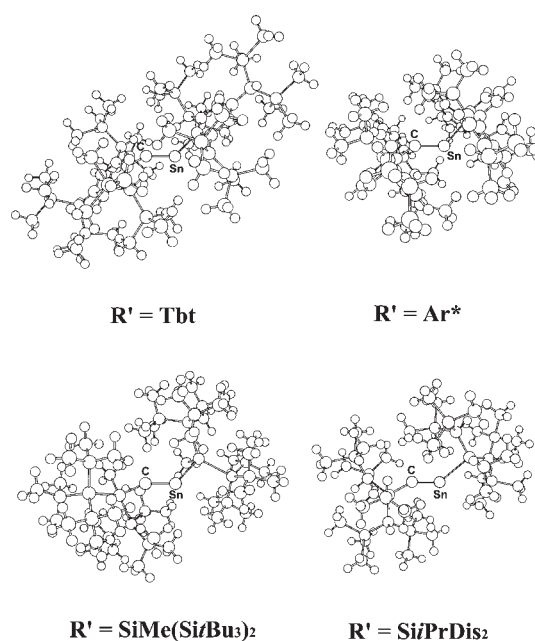


Figure 3. Optimized structures of $R'C\equiv SnR'$ ($R' = Tbt, Ar^*, SiMe(SiBu_3)_2,$ and $Si/PrDis_2$) at the B3LYP/LANL2DZdp level of theory. For details, see the text and Table 2.

consequence, our theoretical investigations demonstrate that the more electropositive the attached ligand R is, the smaller the sum of the ΔE_{DQ} values of the $C-R$ and $Sn-R$ fragments, the more easy hybridization between the central C and Sn elements, the larger the BE of the $RC\equiv SnR$ molecule, the shorter the $C\equiv Sn$ triple-bond distance, and the stronger the predominating central $C\equiv Sn$ triple-bond becomes.

Regarding the stability of $RC\equiv SnR$ bearing the small substituents, we theoretically investigated the potential energy surface of the model $RC\equiv SnR$ ($R = F, H, OH, CH_3,$ and SiH_3) system. This system exhibits a number of stationary points, including three local minima corresponding to $R_2C=Sn:$, $RC\equiv SnR$, and $:C=SnR_2$ and the saddle points connecting them. The transition structures separating the three stable molecular forms involve a successive unimolecular 1,2-migration TS1 (from $RC\equiv SnR$ to $:C=SnR_2$) and a 1,2-migration TS2 (from $RC\equiv SnR$ to $R_2C=Sn:$). The potential energy surfaces calculated at both B3LYP/LANL2DZdp and B3PW91/Def2-QZVP levels with zero-point energy correction for the $RC\equiv SnR$ ($R = F, H, OH, CH_3,$ and SiH_3) model molecules are outlined in Figure 2.

Our theoretical findings based on two DFT levels have denoted that all the triple-bonded $RC\equiv SnR$ species with small substituents are definitely local minima on the singlet potential energy surface. Nevertheless, they are neither kinetically nor thermodynamically stable. From Figure 2, it seems that the effects of small substituents (R) on the relative stabilities of $RC\equiv SnR$ and $R_2C=Sn:$ and of $RC\equiv SnR$ and $:C=SnR_2$ are small. Moreover, our two DFT calculations indicate that these two planar structures featuring the $C=Sn$ double bond exist as minima on the singlet potential energy surface, that is, one of these is $R_2C=Sn:$ which has a lone pair residing on the tin, while the other is $:C=SnR_2$ which has a lone electron pair residing on the carbon. It has to be mentioned that at the computational levels employed in this work, the former structure ($R_2C=Sn:$) is calculated to be the most stable $RC\equiv SnR$ isomer whereas the

latter structure ($:C\equiv SnR_2$) possesses the highest energy of all the minima on the singlet $RC\equiv SnR$ isomerization energy surface. In addition, our computations indicate that the energy difference between $R_2C\equiv Sn$: and $:C\equiv SnR_2$ is at least 47 and 61 kcal/mol for B3LYP and B3PW91 methods, respectively. All the evidence demonstrates that the singlet states of the doubly bonded $C\equiv Sn$ molecules prefer to have the nonbonding electrons residing on the Sn element rather than on the C atom.²² In fact, from the chemical bonding viewpoints, one can ascribe the thermodynamic stability of $R_2C\equiv Sn$: relative to $:C\equiv SnR_2$ to the ability of tin's diffuse electron cloud, which can accommodate a lone electron pair more easily than that on carbon.²² In addition, our theoretical observations point out that the relative stabilities of the three local minima decrease in the order $R_2C\equiv Sn$: > $RC\equiv SnR$ > $:C\equiv SnR_2$. When the reaction is viewed as starting from $:C\equiv SnR_2$, the successive conversions of $:C\equiv SnR_2$ to $RC\equiv SnR$ and $RC\equiv SnR$ to $R_2C\equiv Sn$: are estimated to be from about 55 to 32 (62 to 40) and -56 to -9.1 (-58 to -14) kcal/mol, respectively, at the B3LYP(B3PW91) levels of theory. In other words, the triply bonded structure $RC\equiv SnR$ possessing small substituents seems to be unstable on the singlet energy surface and readily undergoes unimolecular rearrangement to the most stable doubly bonded isomer $R_2C\equiv Sn$:. Owing to proceeding in the endothermic direction, the nondissociative rearrangement $R_2C\equiv Sn$: \rightarrow $RC\equiv SnR$ \rightarrow $:C\equiv SnR_2$ is much more difficult to achieve, with energy barriers of about 57–19 (60–18) and 62–43 (68–47) kcal/mol, respectively, at the B3LYP(B3PW91) levels of theory. As a consequence, our theoretical investigations again demonstrate that the singlet triple-bonded $RC\equiv SnR$ featuring smaller substituents (R) is neither kinetically nor thermodynamically stable with respect to isomerization reactions, that is, the prospects of observing singlet triply bonded $RC\equiv SnR$ (R = F, H, OH, CH₃, and SiH₃) species in a matrix or even as transient intermediates are highly unlikely.

After submitting this paper, one reviewer suggested doing calculations on some pertinent stannaacetylenes with different substituents like $FC\equiv Sn(SiH_3)$ and $(H_3Si)C\equiv SnF$. The B3LYP/LANL2DZdp computational results (kcal/mol) indicate their relative energy ordering is as follows: $:C\equiv Sn(F)(SiH_3)$ (30) > $FC\equiv Sn(SiH_3)$ (0.0) > $(F)(H_3Si)C\equiv Sn$: (-37) and $:C\equiv Sn(F)(SiH_3)$ (54) > $(H_3Si)C\equiv SnF$ (0.0) > $(F)(H_3Si)C\equiv Sn$: (-13). Again, our theoretical observations strongly suggest that using the small substituents cannot greatly stabilize the singlet triply bonded $RC\equiv SnR$ species.

3. Large Ligands on Substituted $R'C\equiv SnR'$. From the above conclusions for the cases of small substituents, bulky substituents are thus expected to destabilize $R_2C\equiv Sn$: and $:C\equiv SnR_2$ relative to $RC\equiv SnR$ because of severe steric congestion. Also, it is reasonable to anticipate that the presence of extremely bulky substituents at both ends of the $RC\equiv SnR$ molecules can protect its triple bond from intermolecular reactions such as dimerization. To examine the effect of bulky substituents, the structures of $R'C\equiv SnR'$ optimized for $R' = Tbt, Ar^*, SiMe(Si^tBu_3)_2,$ and $SiPrDis_2$ (Scheme 1) at the B3LYP/LANL2DZdp level are shown in Figure 3.^{23,24} Also, selected geometrical parameters, doublet–quartet energy splitting for C–R' and Sn–R' fragments (ΔE_{DQ}), natural charge densities on the central carbon and tin elements (Q_C and Q_{Sn}), and binding energies (BE) are collected in Table 2.

According to available experimental data, it was already reported that the C–Sn single-bond²⁰ and C=Sn double-bond²¹ distances are about 2.133–2.372 and 1.982–2.081 Å, respectively.

Table 2. Geometrical Parameters, Doublet–Quartet Energy Splitting (ΔE_{DQ}), Nature Charge Densities (Q_C and Q_{Sn}), and Binding Energies (BE) of $R'C\equiv SnR'$ at the B3LYP/LANL2DZdp Level

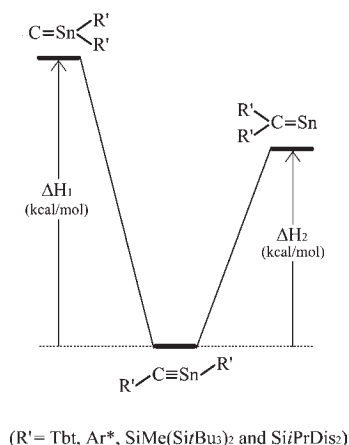
R'	Tbt	Ar*	SiMe(Si ^t Bu ₃) ₂	SiPrDis ₂
B3LYP/LANL2DZdp				
C≡Sn (Å)	1.981	1.965	1.949	1.909
∠R'–C–Sn (deg)	144.9	143.9	154.3	143.9
∠C–Sn–R' (deg)	123.1	129.9	125.7	139.3
∠R'–C–Sn–R' (deg)	178.3	177.2	123.0	131.3
Q_C^a	–1.202	–0.7378	–1.195	–1.303
Q_{Sn}^b	0.4266	0.3271	0.7539	0.3893
ΔE_{DQ} for C (kcal mol ^{–1}) ^c	31.15	30.39	10.72	–1.428
ΔE_{DQ} for Sn (kcal mol ^{–1}) ^d	43.02	48.97	28.47	25.77
BE (kcal mol ^{–1}) ^e	44.17	44.52	50.05	71.76
ΔH_1 (kcal mol ^{–1}) ^f	102.6	84.81	58.27	72.62
ΔH_2 (kcal mol ^{–1}) ^g	76.25	38.95	33.99	35.39
ΔH_a (kcal mol ^{–1}) ^h	125.0	186.7	61.36	48.10
ΔH_b (kcal mol ^{–1}) ⁱ	128.2	134.2	46.88	39.04

^aThe natural charge density on the central carbon atom. ^bThe natural charge density on the central tin atom. ^c $\Delta E_{DQ} = E(\text{quartet state of } C-R') - E(\text{doublet state of } C-R')$. ^d $\Delta E_{DQ} = E(\text{quartet state of } Sn-R') - E(\text{doublet state of } Sn-R')$. ^eBE = $E(\text{doublet state of } C-R') + E(\text{doublet state of } Sn-R') - E(R'C\equiv SnR')$. ^f $\Delta H_1 = E(:C\equiv SnR_2) - E(R'C\equiv SnR')$; see Scheme 2. ^g $\Delta H_2 = E(R'_2C\equiv Sn:) - E(R'C\equiv SnR')$ see Scheme 2. ^h $\Delta H_a = E(\text{head–tail dimer}) - 2E(R'C\equiv SnR')$; see Scheme 3. ⁱ $\Delta H_b = E(\text{head–head dimer}) - 2E(R'C\equiv SnR')$; see Scheme 3.

These experimental bond lengths are longer than our present computational results (1.981–1.909 Å), as given in Table 2. This strongly supports the concept that the central C and Sn elements in the $R'C\equiv SnR'$ ($R' = Tbt, Ar^*, SiMe(Si^tBu_3)_2,$ and $SiPrDis_2$) species are triply bonded. Moreover, the central C≡Sn bond lengths of 1.981 and 1.965 Å calculated for $R' = Tbt$ and Ar^* are on average 0.044 Å longer than those of 1.949 and 1.909 Å calculated for $R' = SiMe(Si^tBu_3)_2$ and $SiPrDis_2$. This strongly implies that the Tbt and Ar^* groups are electronegative whereas the $SiMe(Si^tBu_3)_2$ and $SiPrDis_2$ ligands are electropositive. Supporting evidence comes from the fact that the natural charge densities on the central carbon (Q_C) and tin (Q_{Sn}) atoms are negative and positive, respectively, as shown in Table 2. It has to be mentioned here that the C≡Sn lengths of 1.949 and 1.909 Å for $SiMe(Si^tBu_3)_2$ and $SiPrDis_2$ (Table 2) are considerably shorter than those of 2.081, 2.127, and 1.966 Å for R = F, OH, and CH₃ (Table 1), respectively, despite the steric overcrowding of the $SiMe(Si^tBu_3)_2$ and $SiPrDis_2$ groups. The reason for the short distance of the C≡Sn bond is simply because both $SiMe(Si^tBu_3)_2$ and $SiPrDis_2$ are more electropositive than the small substituent ligands as discussed earlier.²²

Additionally, as one can see in Table 2 and Figure 3, our B3LYP results indicate that the $R'C\equiv SnR'$ species featuring the bulky substituents (R') all adopt a trans-bent geometry. In fact, our B3LYP computations point out that all the C–R' and Sn–R' fragments exhibit the ground doublet state, except for the C– $SiPrDis_2$ unit which has a ground quartet state but with a small doublet–quartet energy difference (ΔE_{DQ}) of only about -1.4 kcal/mol. Accordingly, the interaction mode (mode B) in Figure 1 predominates, leading to the trans-bent structure for $R'C\equiv SnR'$. Again, our B3LYP/LANL2DZdp calculations demonstrate that a linear correlation exists between the C≡Sn

Scheme 2



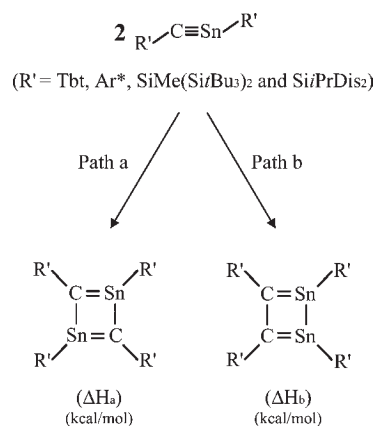
bond distance and the sum of ΔE_{DQ} for the C–R' and Sn–R' fragments, that is, the smaller the sum of ΔE_{DQ} for the C–R' and Sn–R' components, the shorter the C≡Sn bond length and the stronger the C≡Sn bond. From Table 2 it is noteworthy that the sum of ΔE_{DQ} values of 74.2 and 79.4 kcal/mol calculated for R' = Tbt and Ar* are much larger than 39.2 and 24.3 kcal/mol for R' = SiMe(Si*t*Bu₃)₂ and Si*i*PrDis₂. The reason for this is attributed to the electropositive character of the SiMe(Si*t*Bu₃)₂ and Si*i*PrDis₂ groups, which can be used to decrease the size difference between the valence s and p orbitals on the central carbon and tin elements.²²

Basically, it is possible that the R'C≡SnR' species has a tendency to dissociate in solution as the substituent R' becomes bulkier. The binding energy (BE) which is necessary to break the central C≡Sn bond, leaving two ground state units, is predicted to be 44.2, 44.5, 50.1, and 71.8 kcal/mol for R' = Tbt, Ar*, SiMe(Si*t*Bu₃)₂, and Si*i*PrDis₂, respectively, at the B3LYP method. These large BE values imply that the central carbon and tin elements are strongly bonded and that R'C≡SnR' molecules containing bulky substituents will not dissociate in solution, that is, the larger the dissociation energy of the C≡Sn bond, the shorter and stronger the C≡Sn triple bond.

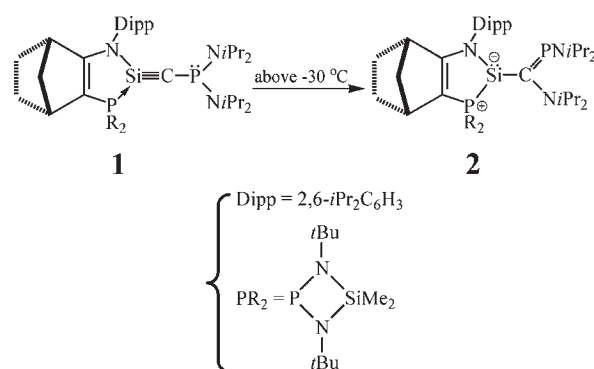
As expected before, bulky groups destabilize the 1,2-R' shifted isomers because they crowd around one end of the central carbon–tin bond. As a result, the bulky substituents (R') can prevent isomerization of R'C≡SnR' compounds, as shown in Scheme 2 and Table 2. Our B3LYP computations demonstrate that the R'C≡SnR' molecules with Tbt, Ar*, SiMe(Si*t*Bu₃)₂, and Si*i*PrDis₂ substituents ΔH_1 and ΔH_2 are 103 and 76.3, 84.8 and 39.0, 58.3 and 34.0, and 72.6 and 35.4 kcal/mol more stable than the 1,2-R' migration isomers, respectively. These computational results suggest that doubly bonded R'₂C=Sn: and :C=SnR'₂ isomers are both kinetically and thermodynamically unstable and will thus rearrange spontaneously to the global minimum R'C≡SnR' triply bonded species, provided severely bulky substituents are employed.

In addition, it is also possible that two R'C≡SnR' molecules could dimerize to form a cyclobutadiene analogue as given in Scheme 3. Our B3LYP computations in Table 2 show that the dimerization reaction enthalpies ΔH_a and ΔH_b are 125 and 128, 187 and 134, 61.4 and 46.9, and 48.1 and 39.0 kcal/mol endothermic for R' = Tbt, Ar*, SiMe(Si*t*Bu₃)₂, and Si*i*PrDis₂, respectively, due to the steric hindrance of the four bulky substituent groups.

Scheme 3



Scheme 4



These energy differences are large enough that such R'C≡SnR' species are unable to undergo polymolecular reactions such as dimerizations. As a consequence, our theoretical investigations indicate that it is crucial to prepare carefully bulky substituent groups in order to make stannacetylene structures stable kinetically and thermodynamically.

Very recently, Kato, Baceiredo, and co-workers reported the isolation and characterization of silyne (**1** in Scheme 4), which is stable up to a temperature of -30 °C.^{6c,d} At temperatures higher than -30 °C the compound is unstable, that is, silyne **1** transforms into the phosphalkene derivative **2** via 1,2-migration of a diisopropylamino group from the phosphine to the central carbon atom. This fascinating synthetic result inspired this study. If silyne **1** can be stabilized as a heteroalkyne ($-C\equiv Si-$), would it be possible to extend this to other triply bonded carbon–tin analogues? In this theoretical work, five typical molecules containing the C≡Sn triple bond were selected as model systems for investigation of their geometric structures when each possesses different pnictogen elements (3–7). The reason for choosing these compounds was that they are all isovalent and might therefore be expected to show similar chemical behavior. The optimized geometries calculated at the B3LYP/LANL2DZ level of theory involving 3–7 are collected in Table 3. From Table 3, it is readily seen that the central C≡Sn bond length is in the range of 2.082–1.992 Å, which compares well with the other available theoretical data as already mentioned in Tables 1 and 2. Moreover, our computations indicate that the C–X (X = N, P, As, Sb,

Table 3. Selected Geometrical Parameters for Molecules (3–7) Containing the C≡Sn Triple Bond Calculated at the B3LYP/LANL2DZ Level of Theory; See Scheme 4

compounds	X = N (3)	X = P (4)	X = As (5)	X = Sb (6)	X = Bi (7)
B3LYP/LANL2DZ					
C≡Sn (Å)	2.060	2.082	2.019	1.992	1.993
C–X (Å)	1.284	1.679	1.796	2.049	2.182
N–Sn (Å)	2.163	2.188	2.172	2.154	2.134
P–Sn (Å)	2.878	2.841	2.871	2.842	2.873
∠N–Sn–C (deg)	107.2	109.8	111.2	114.7	113.7
∠P–Sn–C (deg)	115.3	113.2	113.4	117.4	121.2
∠Sn–C–X (deg)	151.0	161.9	168.7	161.5	165.2
∠C–X–N' (deg)	125.4	114.5	111.1	108.2	103.7
∠C–X–N'' (deg)	128.2	122.3	119.0	110.2	104.2
∠N–Sn–X–N' (deg)	87.13	89.14	94.22	96.42	90.81
∠P–Sn–X–N'' (deg)	36.83	66.36	67.31	68.68	78.33

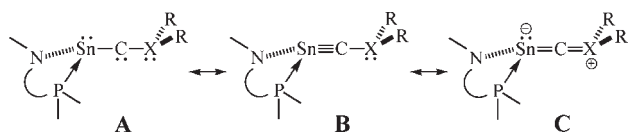


Figure 4. Possible canonical representations for stannaacetylenes 3–7 (X = N, P, As, Sb, and Bi).

and Bi) bond length shows a monotonic increase down the group from N to Bi. For instance, the C–X distance (Å) is predicted to be 1.284 (N), 1.679 (P), 1.796 (As), 2.049 (Sb), and 2.182 (Bi) for the 3, 4, 5, 6, and 7 compounds, respectively. The reason for this is primarily due to the increase of atomic radius of X from nitrogen to bismuth. It has to be emphasized here that these small C–X distances strongly imply multiple-bond character for this bond. Also, it is noted that the $\angle\text{Sn–C–X}$ angle for the 3–7 species is somewhat closed to 180° (about $151\text{--}169^\circ$), which is consistent with our previous computational results as given in Tables 1 and 2. In addition, the strongly bent NSnP ring ($\angle\text{N–Sn–C}$ and $\angle\text{P–Sn–C}$) for all the 3–7 molecules is predicted by our theoretical results as well. All this geometrical information strongly suggests that the molecular structures of 3–7 are better described as the stannaacetylene representation B and the cumulenyl structure C rather than the carbene Lewis base complex structure A as outlined in Figure 4.

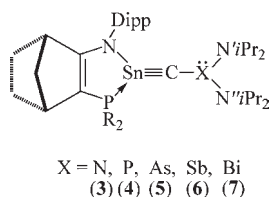


Figure 5. Potential energy surfaces for the 1,2-migration reaction of the 3 (X = N), 4 (X = P), 5 (X = As), 6 (X = Sb), and 7 (X = Bi) molecules calculated at the B3LYP/LANL2DZ level of theory. Relative energies for each stationary point are shown. Hydrogens are omitted for clarity.

the barrier height for the 1,2-migration reaction decreases in the order (kcal/mol) **TS-N-3** (+53.2) > **TS-P-4** (+25.0) > **TS-As-5** (+16.7) > **TS-Sb-6** (+11.8) > **TS-Bi-7** (+3.53). Our theoretical calculations, however, demonstrate that the corresponding reaction enthalpy increase in the order (kcal/mol) **Pro-N-3** (–51.6) < **Pro-Bi-7** (–34.9) < **Pro-P-4** (–21.2) < **Pro-As-5** (–20.8) < **Pro-Sb-6** (–17.9). Accordingly, our theoretical findings strongly suggest that the C≡Sn triply bonded molecules bearing the Sn≡C–N (3), Sn≡C–P (4), or Sn≡C–As (5) skeleton are stable toward an intramolecular 1,2-shift isomerization reaction. It is thus expected that 3, 4, and 5 will soon be successfully isolated and open up a new area in tin chemistry

IV. CONCLUSION

In addition, we examined the potential energy surfaces for the isomerization reactions of compounds 3–7, that is, one diisopropylamino group migrates from the pnictogen element (X) to the carbon atom. To simplify the comparisons and emphasize the trends, we have also given the energies relative to the reactant molecule, which are summarized in Figure 5. As shown in Figure 5,

the barrier height for the 1,2-migration reaction decreases in the order (kcal/mol) **TS-N-3** (+53.2) > **TS-P-4** (+25.0) > **TS-As-5** (+16.7) > **TS-Sb-6** (+11.8) > **TS-Bi-7** (+3.53). Our theoretical calculations, however, demonstrate that the corresponding reaction enthalpy increase in the order (kcal/mol) **Pro-N-3** (–51.6) < **Pro-Bi-7** (–34.9) < **Pro-P-4** (–21.2) < **Pro-As-5** (–20.8) < **Pro-Sb-6** (–17.9). Accordingly, our theoretical findings strongly suggest that the C≡Sn triply bonded molecules bearing the Sn≡C–N (3), Sn≡C–P (4), or Sn≡C–As (5) skeleton are stable toward an intramolecular 1,2-shift isomerization reaction. It is thus expected that 3, 4, and 5 will soon be successfully isolated and open up a new area in tin chemistry

In the present work, we studied the substituent effects of stannaacetylenes using both smaller groups and bulkier substituents by density functional theory. Our theoretical examinations strongly denote that both the kinetic and the thermodynamic stability of the triply bonded RC≡SnR molecule are strongly dependent on the substituents (R). Namely, both the electronic and the steric effects of substituents play a decisive role in making stannaacetylenes synthetically accessible. On the basis of this theoretical study, however, the smaller substituents (such as R = F, H, OH, CH₃, and SiH₃) neither kinetically nor thermodynamically stabilize the triply bonded RC≡SnR species. Nevertheless, our theoretical observations indicate that these triply bonded derivatives are generally stabilized owing to large steric congestion, which prevents their 1,2-R-shifted isomerization, dimerization, or oligomerization. Also, our theoretical investigations suggest that the triply bonded RC≡SnR compounds possessing appropriate bulky substituents, which can surround the central C≡Sn part and protect it to be an isolable species (such as 3, 4, and 5), should make such synthesis in practice a

possibility. We are thus confident that the triply bonded $RC\equiv SnR$ species featuring suitable bulky substituents are intriguing synthetic targets, which is worthy of experimental testing to open a new fundamental area of tin chemistry. We eagerly await experimental results to confirm our predictions.

■ ASSOCIATED CONTENT

S Supporting Information. This material is available free of charge via the Internet at <http://pubs.acs.org>.

■ AUTHOR INFORMATION

Corresponding Author

*E-mail: midesu@mail.ncyu.edu.tw.

■ ACKNOWLEDGMENT

The authors are grateful to the National Center for High-Performance Computing of Taiwan for generous amounts of computing time. They also thank the National Science Council of Taiwan for financial support. Special thanks are also due to Reviewers 1, 2, and 3 for very helpful suggestions and comments.

■ REFERENCES

- (1) For recent reviews, see: (a) Power, P. P. *Chem. Rev.* **1999**, *99*, 3463. (b) Jutzi, P. *Angew. Chem., Int. Ed.* **2000**, *39*, 3797. (c) Weidenbruch, M. *J. Organomet. Chem.* **2002**, *646*, 39. (d) Power, P. P. *Chem. Commun.* **2003**, 2091. (e) Weidenbruch, M. *Angew. Chem., Int. Ed.* **2004**, *43*, 2. (f) Power, P. P. *Appl. Organomet. Chem.* **2005**, *19*, 488. (g) Sekiguchi, A.; Ichinohe, M.; Kinjo, R. *Bull. Chem. Soc. Jpn.* **2006**, *79*, 825. (h) Power, P. P. *Organometallics* **2007**, *26*, 4362 and references therein. (i) Sekiguchi, A. *Pure Appl. Chem.* **2008**, *80*, 447. (j) Sekiguchi, A.; Kinjo, R.; Ichinohe, M. *Synth. Met.* **2009**, *159*, 773. (k) Fischer, R. C.; Power, P. P. *Chem. Rev.* **2010**, *110*, 3877. (l) Peng, Y.; Fischer, R. C.; Merrill, W. A.; Fischer, J.; Pu, L.; Ellis, B. D.; Fettingner, J. C.; Herber, R. H.; Power, P. P. *Chem. Sic.* **2010**, *1*, 461. (m) Sasamori, T.; Han, J. S.; Hironaka, K.; Takagi, N.; Nagase, S.; Tokitoh, N. *Pure Appl. Chem.* **2010**, *82*, 603.
- (2) For $Si\equiv Si$, see: (a) Sekiguchi, A.; Kinjo, R.; Ichinohe, M. *Science* **2004**, *305*, 1755. (b) Wiberg, N.; Vasisht, S. K.; Fischer, G.; Mayer, P. Z. *Anorg. Allg. Chem.* **2004**, *630*, 1823. (c) Sasamori, T.; Hironaka, K.; Sugiyama, T.; Takagi, N.; Nagase, S.; Hosoi, Y.; Furukawa, Y.; Tokitoh, N. *J. Am. Chem. Soc.* **2008**, *130*, 13856.
- (3) For $Ge\equiv Ge$, see: (a) Stender, M.; Phillips, A. D.; Wright, R. J.; Power, P. P. *Angew. Chem., Int. Ed.* **2002**, *41*, 1785. (b) Stender, M.; Phillips, A. D.; Power, P. P. *Chem. Commun.* **2002**, 1312. (c) Pu, L.; Phillips, A. D.; Richards, A. F.; Stender, M.; Simons, R. S.; Olmstead, M. M.; Power, P. P. *J. Am. Chem. Soc.* **2003**, *125*, 11626. (d) Sugiyama, Y.; Sasamori, T.; Hosoi, Y.; Furukawa, Y.; Takagi, N.; Nagase, S.; Tokitoh, N. *J. Am. Chem. Soc.* **2006**, *128*, 1023. (e) Spikes, G. H.; Power, P. P. *Chem. Commun.* **2007**, 85.
- (4) For $Sn\equiv Sn$, see: Phillips, A. D.; Wright, R. J.; Olmstead, M. M.; Power, P. P. *J. Am. Chem. Soc.* **2002**, *124*, 5930.
- (5) For $Pb\equiv Pb$, see: Pu, L.; Twamley, B.; Power, P. P. *J. Am. Chem. Soc.* **2000**, *122*, 3524. However, from a purely geometrical perspective, the lead–lead bond in this experimental work appears to be best characterized as a single bond, i.e., more consistent with a diplumblylene form.
- (6) For $C\equiv Si$, see: (a) Apeloig, Y.; Karni, M. *Organometallics* **1997**, *16*, 310. (b) Karni, M.; Apeloig, Y.; Schröder, D.; Zummack, W.; Rabazzana, R.; Schwarz, H. *Angew. Chem., Int. Ed.* **1999**, *38*, 311. (c) Danovich, D.; Ogiaro, F.; Karni, M.; Apeloig, Y.; Cooper, D. L.; Shaik, S. *Angew. Chem., Int. Ed.* **2001**, *40*, 4023. (c) Gau, D.; Kato, T.; Saffon-Merceron, N.; Cózar, A. D.; Cossío, F. P.; Baceiredo, A. *Angew. Chem., Int. Ed.* **2010**, *49*, 6585. (d) Lühmann, N.; Müller, T. *Angew. Chem., Int. Ed.* **2010**, *49*, 10042.
- (7) For $C\equiv Ge$, see: (a) Bibal, C.; Mazières, S.; Gornitzka, H.; Couret, C. *Angew. Chem., Int. Ed.* **2001**, *40*, 952. (b) Liao, H. -Y.; Su, M.-D.; Chu, S.-Y. *Inorg. Chem.* **2000**, *39*, 3522. (c) Liao, H. -Y.; Su, M.-D.; Chu, S.-Y. *Chem. Phys. Lett.* **2001**, *341*, 122.
- (8) For $C\equiv Sn$, see: (a) Setaka, W.; Hirai, K.; Tomioka, H.; Sakamoto, K.; Kira, M. *J. Am. Chem. Soc.* **2004**, *126*, 2696. In this work, Kira and co-workers reported the $C\equiv Sn$ triple-bond length in the $HC\equiv SnH$ molecule, which was calculated to be 2.016, 1.936, 1.922, and 1.986 Å at QCISD/3-21G*, MP2/3-21G*, CCD/3-21G*, and B3LYP/3-21G* levels of the theory, respectively. (b) Setaka, W.; Hirai, K.; Tomioka, H.; Sakamoto, K.; Kira, M. *Chem. Commun.* **2008**, 6558.
- (9) It should be mentioned that the electronegativity decreases in the order $C(2.5) > Sn(1.7)$, see: Allred, A. L. *J. Inorg. Nucl. Chem.* **1961**, *17*, 215 and references cited therein.
- (10) For instance, see: (a) Schubert, U.; Grubert, S.; Schulz, U.; Mock, S. *Organometallics* **1992**, *11*, 3163. (b) Buffin, B. P.; Poss, M. J.; Arif, A. M.; Richmond, T. G. *Inorg. Chem.* **1993**, *32*, 3805. (c) Pinkes, J. R.; Cutler, A. R. *Inorg. Chem.* **1994**, *33*, 759. (d) Yosida, J.; Izawa, M. *J. Am. Chem. Soc.* **1997**, *119*, 9361. (e) Blumenstein, M.; Schwarzkopf, K.; Metzger, J. O. *Angew. Chem., Int. Ed. Engl.* **1997**, *36*, 325. (f) Davis, S. R.; Chadwick, A. V.; Wright, J. D. *J. Mater. Chem.* **1998**, *8*, 2065. (g) Schwarzkopf, K.; Blumenstein, M.; Hayen, A.; Metzger, J. O. *Eur. J. Org. Chem.* **1998**, 177. (h) Cheng, X.; Slobodnick, C.; Deck, P. A. *Inorg. Chem.* **2000**, *39*, 4921. (i) Fugami, K.; Kawata, K.; Enokido, T.; Mishiba, Y.; Hagiwara, S.; Hirunuma, Y.; Koyama, D.; Kameyama, M.; Kosugi, M. *J. Organomet. Chem.* **2000**, *611*, 433. (j) Wakabayashi, K.; Yorimitsu, H.; Shinokubo, H.; Oshima, K. *Org. Lett.* **2000**, *2*, 1899. (k) Grushin, V. V.; Marshall, W. J.; Thorn, D. L. *Adv. Synth. Catal.* **2001**, *343*, 433. (l) Qiu, L.; Pol, V. G.; Wei, Y.; Gedanken, A. *New J. Chem.* **2004**, *28*, 1056. (m) Uenoyama, Y.; Fukuyama, T.; Nobuta, O.; Matsubara, H.; Ryu, I. *Angew. Chem., Int. Ed.* **2005**, *44*, 1075. (n) Ballivet-Tkatchenko, D.; Chermette, H.; Plasseraud, L.; Walter, O. *Dalton Trans.* **2006**, 5167. (o) Wang, Y.; Lee, J. Y. *Angew. Chem., Int. Ed.* **2006**, *45*, 7039. (p) Kim, S.; Lim, K.-C.; Kim, S.; Ryu, I. *Adv. Synth. Catal.* **2007**, *349*, 527. (q) Fischer, A.; Jun, Y.-S.; Thomas, A.; Antonietti, M. *Chem. Mater.* **2008**, *20*, 7383. (r) Zabala, A. V.; Pape, T.; Hepp, A.; Schappacher, F. M.; Rodewald, U. Ch.; Pöttgen, R.; Hahn, F. E. *J. Am. Chem. Soc.* **2008**, *130*, 5648. (s) Qiu, Y.; Yan, K.; Yang, S. *Chem. Commun.* **2010**, 46, 8359.
- (11) Frisch, M. J.; Trucks, G. W.; Schlegel, H. B.; Scuseria, G. E.; Robb, M. A.; Cheeseman, J. R.; Zakrzewski, V. G.; Montgomery, Jr., J. A.; Vreven, T.; Kudin, K. N.; Burant, J. C.; Millam, J. M.; Iyengar, S. S.; Tomasi, J.; Barone, V.; Mennucci, B.; Cossi, M.; Scalmani, G.; Rega, N.; Petersson, G. A.; Nakatsuji, H.; Hada, M.; Ehara, M.; Toyota, K.; Fukuda, R.; Hasegawa, J.; Ishida, M.; Nakajima, T.; Honda, Y.; Kitao, O.; Nakai, H.; Klene, M.; Li, X.; Li, J. E.; Hratchian, H. P.; Cross, J. B.; Adamo, C.; Jaramillo, J.; Gomperts, R.; Stratmann, R. E.; Yazyev, O.; Austin, A. J.; Cammi, R.; Pomelli, C.; Ochterski, J. W.; Ayala, P. Y.; Morokuma, K.; Voth, G. A.; Salvador, P.; Dannenberg, J. J.; Zakrzewski, V. G.; Dapprich, S.; Daniels, A. D.; Strain, M. C.; Farkas, O.; Malick, D. K.; Rabuck, A. D.; Raghavachari, K.; Foresman, J. B.; Ortiz, J. V.; Cui, Q.; Baboul, A. G.; Clifford, S.; Cioslowski, J.; Stefanov, B. B.; Liu, G.; Liashenko, A.; Piskorz, P.; Komaromi, I.; Martin, R. L.; Fox, D. J.; Keith, T.; Al-Laham, M. A.; Peng, C. Y.; Nanayakkara, A.; Challacombe, M.; Gill, P. M. W.; Johnson, B.; Chen, W.; Wong, M. W.; Gonzalez, C.; Pople, J. A. *Gaussian 03*; Gaussian, Inc.: Wallingford, CT, 2003.
- (12) (a) Becke, A. D. *Phys. Rev. A* **1988**, *38*, 3098. (b) Becke, A. D. *J. Chem. Phys.* **1993**, *98*, 5648.
- (13) Lee, C.; Yang, W.; Parr, R. G. *Phys. Rev. B* **1988**, *37*, 785.
- (14) Perdew, J. P.; Wang, Y. *Phys. Rev.* **1992**, *B45*, 13244.
- (15) (a) Dunning, T. H., Jr.; Hay, P. J. In *Modern Theoretical Chemistry*; Schaefer, H. F., III, Ed.; Plenum: New York, 1976; pp 1–28. (b) Hay, P. J.; Wadt, W. R. *J. Chem. Phys.* **1985**, *82*, 270. (c) Hay, P. J.; Wadt, W. R. *J. Chem. Phys.* **1985**, *82*, 284. (d) Hay, P. J.; Wadt, W. R. *J. Chem. Phys.* **1985**, *82*, 299.
- (16) Check, C. E.; Faust, T. O.; Bailey, J. M.; Wright, B. J.; Gilbert, T. M.; Sunderlin, L. S. *J. Phys. Chem. A* **2001**, *105*, 8111.
- (17) Weigend, F.; Ahlrichs, R. *Phys. Chem. Chem. Phys.* **2005**, *7*, 3297.

(18) For the quartet state of the monomer, there must be an sp hybridization. Namely, one sp orbital is used for bonding with R, while the three unpaired electrons are in the two p and one sp orbitals.

(19) The sum of the covalent radii of C and Sn is 2.170 Å, see: Greenwood, N. N.; Earnshaw, A. *Chemistry of the Elements*; Pergamon: Oxford, England, 1984; p 430.

(20) For instance, see: (a) Batsanov, A. S.; Howard, J. A. K.; Brown, M. A.; McGarvey, B. R.; Tuck, D. G. *Chem. Commun.* **1997**, 699. (b) Cardin, C. J.; Cardin, D. J.; Constantine, S. P.; Drew, M. G. B.; Rashid, H.; Convery, M. A.; Fenske, D. *Dalton Trans.* **1998**, 2749. (c) Davenport, A. J.; Davies, D. L.; Fawcett, J.; Russell, D. R. *Dalton Trans.* **2002**, 326. (d) Wills, C.; Izod, K.; Clegg, W.; Harrington, R. W. *Dalton Trans.* **2010**, 39, 2379.

(21) For instance, see: (a) Anselme, G.; Ranaivonjatovo, H.; Escudié, J.; Couret, C.; Satgé, J. *Organometallics* **1992**, *11*, 2748. (b) Weidenbruch, M.; Kilian, H.; Stürmann, M.; Pohl, S.; Saak, W.; Marsmann, H.; Steiner, D.; Berndt, A. *J. Organomet. Chem.* **1997**, *530*, 255. (c) Escudié, J.; Couret, C.; Ranaivonjatovo, H. *Coord. Chem. Rev.* **1998**, *178*, 565. (d) Lee, V. Ya.; Sekiguchi, A. *Organometallics* **2004**, *23*, 2822. (e) Mizuhata, Y.; Takeda, N.; Sasamori, T.; Tokitoh, N. *Chem. Commun.* **2005**, 5876. (f) Mizuhata, Y.; Sasamori, T.; Takeda, N.; Tokitoh, N. *J. Am. Chem. Soc.* **2006**, *128*, 1050. (g) Mizuhata, Y.; Sasamori, T.; Nagahora, N.; Watanabe, Y.; Furukawa, Y.; Tokitoh, N. *Dalton Trans.* **2008**, 4409. (h) Fatah, A.; Ayoubi, R. E.; Gornitzka, H.; Ranaivonjatovo, H.; Escudié, J. *Eur. J. Chem.* **2008**, 2007. (i) Mizuhata, Y.; Tokitoh, N. *Appl. Organometal. Chem.* **2010**, *24*, 902.

(22) (a) Pyykkö, P.; Desclaux, J.-P. *Acc. Chem. Res.* **1979**, *12*, 276. (b) Kutzelnigg, W. *Angew. Chem., Int. Ed. Engl.* **1984**, *23*, 272. (c) Pyykkö, P. *Chem. Rev.* **1988**, *88*, 563. (d) Pyykkö, P. *Chem. Rev.* **1997**, *97*, 597.

(23) The reason for choosing these four bulky ligands (Scheme 1) is based on the conclusions reported by Nagase et al. It was found that the SiMe(Si^tBu₃)₂ and SiⁱPrDis₂ groups are electropositive, while Tbt and Ar* are electronegative, as indicated by natural charge densities. Moreover, these ligands have already been successfully synthesized by experiments. Therefore, they have been suggested as sterically promising substituents. Also see ref 24.

(24) For instance, see: (a) Kobayashi, K.; Nagase, S. *Organometallics* **1997**, *16*, 2489. (b) Nagase, S.; Kobayashi, K.; Takagi, N. *J. Organomet. Chem.* **2000**, *611*, 264. (c) Kobayashi, K.; Takagi, N.; Nagase, S. *Organometallics* **2001**, *20*, 234. (d) Takagi, N.; Nagase, S. *Organometallics* **2001**, *20*, 5498. (e) Takagi, N.; Nagase, S. *Chem. Lett.* **2001**, 966. (f) Takagi, N.; Nagase, S. *Eur. J. Inorg. Chem.* **2002**, 2775.